P-36

NASA Technical Memorandum 100169

Materials for Engine Applications Above 3000 °F—an Overview

Nancy J. Shaw, James A. DiCarlo, Nathan S. Jacobson, Stanley R. Levine, James A. Nesbitt, Hubert B. Probst, William A. Sanders, and Carl A. Stearns
Lewis Research Center
Cleveland, Ohio

October 1987

Date for general release October 1989

NASA

MATERIALS FOR ENGINE APPLICATIONS ABOVE 3000 °F - AN OVERVIEW

Nancy J. Shaw, James A. DiCarlo, Nathan S. Jacobson, Stanley R. Levine,
James A. Nesbitt, Hubert B. Probst, William A. Sanders,
and Carl A. Stearns
National Aeronautics and Space Administration
Lewis Research Center
Cleveland, Ohio 44135

E-3734

SUMMARY

Materials for future generations of aeropropulsion systems will be required to perform at ever-increasing temperatures and have properties superior to the current state of the art. Improved engine efficiency can reduce specific fuel consumption and thus increase range and lower operating costs. The ultimate payoff gain is expected to come when materials are developed that can perform without cooling at gas temperatures to 2200 °C (4000 °F). This report presents an overview of materials for applications above 1650 °C (3000 °F), some pertinent physical property data, and the rationale used (1) to arrive at recommendations of material systems that qualify for further investigation, and (2) to develop a proposed plan of research. From an analysis of available thermochemical data it was concluded that such materials systems must be composed of oxide ceramics. The required structural integrity will be achieved by developing these materials into fiber-reinforced ceramic composites.

INTRODUCTION

Materials for future generations of aeropropulsion systems will be required to perform at ever-increasing temperatures and have properties superior to the current state of the art. The general scenerio is indicated in figure 1, where the operating temperature regimes for various aeropropulsion systems are shown as a function of required operating time. For aircraft engines the drive is to increase temperature capability and extend operating life. In both the commercial and military aircraft engine contexts, these goals derive from the desire to improve engine performance while reducing operating costs. Improved engine efficiency can reduce specific fuel consumption and thus increase range and lower operating costs. Additional savings of dollars and time also result from the ability to achieve greater speed. These payoffs can be attained by operating at higher gas temperatures, by reducing the cooling air needed to keep the materials of various components within their temperature capabilities, and by reducing the weight of the propulsion system. Considerable research and development effort is being expended to provide lighter weight materials that can sustain long-duration exposure to temperatures of 1650 °C (3000 °F) in high-velocity-flow oxidizing environments. Although developing such materials certainly presents challenges, potentially viable candidate material systems exist, as evidenced by the variety of research and development projects currently being pursued.

Attaining this ambitious goal will yield high payoffs, but the ultimate payoff is expected to come when materials are developed that can perform without cooling at gas temperatures between 1650 and 2200 °C (3000 and 4000 °F). This situation is considerably more speculative. At present, carbon-carbon

composites are the only materials receiving extensive attention. Although they are lightweight and have attractive mechanical properties at these ultrahigh temperatures, carbon/carbon composites are susceptible to severe oxidative degradation and this presents formidable problems. An obvious way to combat this inadequate environmental durability is to develop coatings that will provide the necessary oxidation resistance and, indeed, this route is being pursued vigorously by many research organizations. Although progress has been made on this front, no completely satisfactory coating system has been demonstrated for long-duration use. Coatings have been developed that perform reasonably well for relatively short times for non-human-rated applications under very special operating conditions. However, even for the best coatings so far developed, life prediction has been elusive. This stems mainly from the fact that coatings generally possess flaws that ultimately limit their lives. Thus for long-duration cyclic use and human-rated applications, coatings for carbon-carbon are still considered to be extremely risky. A viable coating for carbon-carbon must be "prime reliant" (i.e., it must guarantee protection for a substrate that would catastrophically fail under use conditions without a coating). Furthermore coatings add weight; if a suitable coating system is developed, it might be sufficiently heavy to negate the desirable weight advantage of carbon-carbon. On the basis of these considerations, it seems prudent to look for alternative material systems for use above 1650 °C (3000 °F).

This study assessed what is currently known about such materials and identified potential candidate engine system materials for long-duration use. This report presents an overview of materials for applications above 1650 °C (3000 °F), some pertinent physical property data, and the rationale used (1) to arrive at recommendations of material systems that qualify for further investigation and (2) to develop a proposed plan of research.

BACKGROUND

The current major emphasis in the development of materials for high-temperature (<1650 °C (3000 °F)) use is directed at carbon/carbon, silicon carbide, and silicon nitride composite systems. For ultra-high-temperature (>1650 °C (3000 °F)) use silicon-based systems are not viable candidates in oxidizing environments because, as shown later, their oxidation characteristics limit their upper use temperature to about 1650 °C (3000 °F). Carbon/carbon composites possess adequate mechanical properties at ultrahigh temperatures as noted earlier but require coatings for use in oxidizing environments. Extensive effort is being expended to develop coatings for carbon/carbon composites. The inherent risks associated with the use of coatings have been identified, but suitable coating systems for long-duration cyclic use at ultrahigh temperatures in high-velocity oxidizing flows have yet to be demonstrated.

Recent review articles by Fleischer (ref. 1) and Hillig (ref. 2) proved helpful in that they focus on critical material characteristics. Properties such as melting (or dissociation) temperature, specific gravity, Young's modulus, strength, creep resistance, and thermal expansion are addressed as being especially important. Beyond these properties, environmental stability is highlighted as the most important requirement, with special emphasis given to oxidation resistance. This, together with fundamental thermodynamic considerations of chemical reactions (based in many cases on necessarily extrapolated thermochemical data), ultimately led Hillig to consider only oxides to

be viable composite matrices or monolithic ceramics for applications in air to 2100 °C (3800 °F).

Morrell's handbook (ref. 3) compares limiting material use temperatures in regard to melting temperatures, dimensional stability, creep, and oxidation and provides some helpful background information. Also of value are the material property compilations from the Battelle Memorial Institute series (refs. 4 to 7), the volume on high-temperature oxides edited by Alper (ref. 8), and Shaffer's (ref. 9) handbook on high-temperature materials.

We have been especially cognizant of the current U.S. Air Force program dealing with ultra-high-temperature engine materials and the particulars of the 12 current material screening contracts funded by the Air Force.[1] These contracts are directed at identifying and developing materials for use above 1650 °C (3000 °F). Eight of the contracts take the ceramic matrix composite approach, where the matrix is usually an oxide and the reinforcing second phase is a carbide, boride, or nitride. Fiber matrix compatibility and microstructural stability are apparently the major concerns, but environmental durability is also receiving consideration. The other four contracts focus on protective coatings for carbon/carbon composites. The approach here is to develop coating systems that are layered structures of various materials including silicon carbide, hafnium carbide, titanium carbide, and iridium alloys. Coating systems are evaluated primarily by oxidation testing.

Considerable research effort is being expended to develop monolithic ceramic materials for use in advanced heat engine applications to 1650 °C (3000 °F). The primary candidate materials are silicon carbide (SiC), silicon nitride (Si_3N_4), and partially stabilized zirconia (PSZ). Although Si_3N_4 and PSZ are stronger than SiC, their strength degrades above ~1200 °C (2200 °F). SiC, on the other hand, retains its strength to nearly 1480 °C (2700 °F). As discussed later, both SiC and Si_3N_4 suffer from oxidation problems above ~1650 °C (3000 °F).

In spite of recent successes in producing monolithic bodies of these materials with increased strength, SiC, Si_3N_4, and PSZ still have a major limitation in their inherent brittleness, which can lead to catastrophic failure. This limitation is being addressed by developing toughening schemes based on the use of either short or continuous fibers. Such composites as carbon/carbon (C/C), SiC/glass ceramic, SiC/SiC, and SiC/Si_3N_4 have demonstrated better fracture strength, thermal shock resistance, and fracture toughness than monolithics. As already noted, C/C materials are totally dependent on protective coatings. The glass ceramic systems are limited in temperature capability to ~1315 °C (2400 °F). Therefore the most attractive candidates for use to 1650 °C (3000 °F) are ceramic composite systems that use SiC reinforcing fibers in a silicon-nitride- or silicon-carbide-based matrix. Commercially available SiC/SiC composites, as well as most composites under development, use the Nicalon[2] SiC fiber, which is appropriately coated (usually with chemically

---

[1]Program Review, Materials and Process Screening PRDA, Wright-Patterson Air Force Base, Ohio, December 9-10, 1986.

[2]Nicalon is a trade name for an SiC fiber made by Nippon.

vapor deposited SiC), to toughen a composite by developing a weak interfacial bond between the fiber and the matrix. One example of this type of composite, the one-dimensional Société Européene de Propulsion CERASEP, has room-temperature strength of ~410 MPa (60 ksi); however, this strength decreases to ~240 MPa (35 ksi) at ~1200 °C (2200 °F). This strength decrease is consistent with the expected behavior of Nicalon, which is subject to thermal instability due to oxygen and excess carbon in the microstrucutre. Surmounting this limitation of Nicalon is being actively pursued, along with other fiber developments, by many organizations.

In the final analysis the prospects look promising for developing fiber-reinforced ceramic composites with use temperatures near 1650 °C (3000 °F). Other composite systems will have to be conceived and developed for use above 1650 °C (3000 °F) because silicon-based systems cannot be expected to survive above this temperature. This reality derives from fundamental thermochemical considerations. Worrell[1] demonstrated this graphically. An appreciation of the situation can be gained by examining the data presented herein as figures 2 and 3. The silicon-based systems derive their limited oxidation resistance from the development of a protective silica (SiO_2) scale. Volatile vapor species also form to maintain thermodynamic equilibrium; as can be seen from the figures, the SiO and N_2 pressures or CO and SiO pressures at the oxide/ceramic interfaces for the respective Si_3N_4 or SiC systems reach 1 atm at ~1800 °C (3300 °F), causing cracking and spalling of the protective SiO_2 scale. This intrinsic thermodynamic limit would in practice not be expected to be the real limit because variations in composition probably would lower the temperature at which 1-atm total vapor pressure at the interface is obtained. Additionally, detrimental bubble formation would likely take place at an even lower temperature. Therefore, the maximum use temperature of 1650 °C (3000 °F) for silicon-based systems appears to be an optimistic limit. And thus current state-of-the-art ceramic composite systems do not offer any potential for use above this temperature.

Research in high-temperature chemistry began to flourish in the early 1950's when scientists recognized the significance of the work of Brewer and his associates. The decade of the 1960's was particularly fruitful, and the work of this era provides most of the pertinent data presently available. Since the early 1970's, research in high-temperature chemistry has declined significantly for various (but scientifically unacceptable) reasons. This fact can be readily appreciated by noting the publication dates of the references cited in this report. Today, when there is an urgent need for additional high-temperature chemistry data, much of the expertise has been lost. Renewed efforts in this area are required to provide the fundamental information needed to cope with anticipated high-temperature materials technology. This situation has made the study reported herein, as well as similar work of others, particularly difficult. The complete lack of data for certain materials and the incomplete state of much of the available data have made it impossible to predict with any certainty the thermochemical stability of many potential ultra-high-temperature materials. Although our study has by no means been exhaustive, we feel that the data presented are a good representation of the best available. We have avoided, as much as possible, extrapolating existing data, have made no assumptions regarding congruency in vaporization, and have not

---

[1]Program Review, Materials and Process Screening PRIDA, Wright-Patterson Air Force Base, Ohio, December 9-10, 1987.

made judgments about conflicting data. For a definitive study more work must be done.

In the course of our study we became painfully aware of the paucity of high-temperature data for many materials. This is particularly true in regard to thermodynamic data. Most thermochemical data required to determine the high-temperature stability of materials derive from the research area generally termed "high temperature chemistry." In broad terms this field of endeavor deals mainly, but not exclusively, with the chemical and physical nature of high-temperature vapors. Investigations in this area establish the nature of high-temperature chemical reactions, the nature and energetics of chemical bonding, and the thermodynamic properties of solids, liquids, and gases. High-temperature chemists have ingeniously applied nearly every kind of experimental apparatus to elucidate the chemistry of materials in the high-temperature regime. Building on the early work of Hertz, Knudsen, and Langmuir, they have provided vapor pressure data, dissociation energies, and thermodynamic data for a broad range of materials that find applications at high temperatures. Although their work has been prolific, there still remains a paucity of data.

SELECTION CRITERIA

The following general selection criteria were established on the basis of the knowledge we acquired from the general literature and our experience in high-temperature structural materials:

(1) Mechanical and microstructural stability
  (a) Melting (decomposition) temperatures above 2000 °C (3600 °F)
  (b) Absence of phase transformations
  (c) Low atomic and dislocation mobility (creep rate or grain growth rate versus temperature)
  (d) Thermal shock resistance (shock factor R)
  (e) High initial ratio of strength to stiffness (specific modulus E/ρ)

(2) Environmental stability
  (a) Surface recession due to volatility
  (b) Surface recession due to oxidation

(3) Nonhazardousness in fabrication or use (nonradioactive and nontoxic)

In order to operate above 1650 °C (3000 °F), a material must be a solid and have sufficient structural integrity to meet intended use applications. Thus as a first consideration a material's melting temperature T_m, or decomposition temperature T_d, must be sufficiently high. A minimum of 2000 °C (3600 °F) was chosen as the initial property requirement.

Second, a material must maintain its mechanical stability for extended times at temperature and during thermal cycling. This implies no significant plasticity or atomic diffusion and, of course, no deleterious phase changes. Good thermal shock resistance is also a must. Because metals and metallic alloys display considerable atomic diffusion at about $0.6T_m$ (even tungsten, with a T_m of 3410 °C (6170 °F) shows mechanical instability at ~1300 °C (2400 °F), these materials were essentially eliminated from consideration.

Third, a material must possess sufficient environmental resistance to withstand the gas conditions and temperatures typical of those anticipated in advanced aeropropulsion systems. A material therefore should not undergo any significant long-term surface degradation in high-temperature oxidizing environments. This requirement immediately eliminates from consideration all materials that react with oxygen to form volatile products. Such materials would include, but not be limited to, carbon, boron, and the refractory metals.

Finally, to avoid the handling of hazardous materials and the attendent problems associated with their processing, we decided that all materials that contained radioactive elements or had any propensity to evolve toxic gases would be eliminated from consideration.

The general class of materials remaining after application of these criteria is ceramics, which in bulk monolithic form typically display brittle fracture, low fracture toughness, and poor thermal shock resistance. An engineering approach that can significantly mitigate these deleterious effects involves creating composite structures in which a ceramic matrix is reinforced by a high-strength, continuous ceramic fiber. Indeed, Bhatt (ref. 10) at the NASA Lewis Research Center and researchers at other laboratories have made ceramic matrix composites (CMC) that at temperatures to 1300 °C (2400 °F) demonstrate metal-like graceful failure, insensitivity to crack size, and significantly better thermal shock behavior than the unreinforced matrix material. For this reason, we believe that if a ceramic material can be identified that has the required environmental and mechanical stability above 1650 °C (3000 °F), ceramic composites with optimum structural performance could probably be engineered. Such engineering would be based on placing a ceramic fiber in the same type of ceramic matrix. Current experience has shown that, because flaws are minimized during processing, ceramics can be significantly stronger in fiber form than in bulk form. The engineering challenge would be to produce the fiber and make it compatible with the matrix.

In summary, establishing general selection criteria focused attention on high-temperature ceramic materials such as oxides, carbides, borides, and nitrides. We anticipated that to maintain structural reliability these materials would be processed into ceramic matrix composites.

The next step was then to rank candidate materials according to their probability of success as structural materials with the necessary high-temperature capability. To accomplish this, we acquired property data from the literature (appendix A). The properties needed for evaluation were ranked according to the two primary selection criteria, mechanical and environmental stability.

Mechanical stability is related to microstructural stability. These properties can be measured by the absence of phase transformations and such parameters as creep strain or grain growth as a function of temperature and stress. These parameters are a measure of the existence of internal-defect-controlled processes that can eventually result in time-dependent mechanical failure. Also related to mechanical stability is the ability to survive thermal shock conditions. For brittle materials thermal shock degradation is minimal in materials with high R values, where $R = \sigma\tau/\alpha$ and σ is the material strength, τ is the thermal conductivity, and α is the thermal expansion coefficient. For structural applications in airborne turbine engines it is desirable that,

besides mechanical stability, potential ceramic materials also have high specific strength and high specific stiffness. Because stiffness is measured by Young's modulus E and since the strength of a brittle material generally increases with modulus, this requirement reduces to ranking materials according to their specific modulus ratio E/ρ, where ρ is material density.

Because of the oxidative environments anticipated in advanced gas turbine engines, the first key issue is surface stability in oxygen partial pressures ranging from near zero to many atmospheres. As discussed later, this property can be quantified in terms of vapor pressure and oxidation-induced surface recession rates as a function of temperature.

SURFACE STABILITY

Volatility

At high temperatures volatility is a major criterion for assessing the suitability of materials. Vapor pressure data provide a quantitative measure of volatility. Because vapor pressures are measured in a vacuum under equilibrium conditions, one might inquire, in the context of the present study, what bearing this has on materials operating in the elevated-pressure environment of turbine engines. However, it must be recalled that this environment is also characterized by high-velocity flow. High flow velocity increases the mass transfer coefficient, which governs the mass flux rate at which gaseous species escape across the boundary layer present as a result of the system pressure. For sufficiently high velocities this mass flux rate can approach the equilibrium value, which is the maximum possible rate. Lowell (ref. 11) and Stearns (ref. 12) show this to be the case for velocities typical of turbine engines. Thus vapor pressure data are relevant to the considerations of this study in that they measure the worst-case rate of material loss.

Vapor pressure data for a variety of high-temperature materials are presented in figures 4 to 7. These data were taken from several compendia and original sources (refs. 13 to 23). It should be recognized that most solids do not vaporize as a single molecular species - often the vapor consists of multiple species. If the net vapor composition is the same as the solid composition, the solid composition will not change with time and the solid is said to vaporize congruently. However, if the net vapor composition is different from the solid composition, as is often the case, the solid composition will change with time and the solid is said to vaporize incongruently. This change in composition, in addition to material loss by vaporization, can also be an important degradation route for materials at high temperature. Table I lists the major vapor species for the materials covered by figures 4 to 7. It must be stressed here that no attempt was made to critically review available data since the purpose was only to roughly estimate the volatilities of some candidate materials.

To provide more relevance to the vapor pressure data, we calculated mass flux rates per unit surface area J with the Hertz-Langmuir equation given by

$$J_i = \frac{P_i}{(2M_i \pi RT)^{1/2}}$$

or

$$J_i(g/cm^2\ hr) = 1.6\times10^5 P_i\left(\frac{M_i}{T}\right)^{1/2}$$

where P_i is the vapor pressure of species i, expressed in atmospheres, M_i is the molecular weight of species i, R is the gas constant, and T is the temperature in degrees Kelvin. Maximum vapor fluxes at 2200 K (3500 °F) for materials of interest here are tabulated in appendix A. The term M_i was calculated by assuming equal contributions of the respective vapor species for each material listed in table I, and the vapor pressures of the individual species were summed. Another meaningful measure of material vaporization behavior is the recession rate R_r, which can be calculated for a congruently or nearly congruently vaporizing material by the expression

$$R_r(\mu m/hr) = 10^4\,\frac{J}{\rho} = \frac{1.6\times10^9 P}{\rho}\left(\frac{M}{T}\right)^{1/2}$$

where ρ is the density in grams per cubic centimeter.

If we expect that an engine component should operate for at least 1000 hr without detrimental degradation, a recession of 10 mils is reasonable to assume. This translates to a rate of 0.25 μm/hr. Putting this value into the preceding equation and rearranging gives

$$\frac{P}{\rho}\left(\frac{M_i}{T}\right)^{1/2} = 1.6\times10^{-10}$$

For a wide variety of materials of consideration here, the quantity $M_i^{1/2}/\rho$ varies between 1 and 2, and this equation becomes approximately

$$\frac{P}{T^{1/2}} = 10^{-10}$$

For temperatures from 1900 to 2500 K (3000 to 4000 °F) this yields a pressure P of ~5×10^{-9} atm. Thus for a congruently vaporizing material to have the assumed acceptable recession rate of 0.25 μm/hr, its vapor pressure must be roughly 5×10^{-9} atm or less.

In general, materials that meet the vaporization criteria will be found in the lower left corners of figures 4 to 7. Examining the data for oxides (figs. 4 and 5 and table I) reveals some clear trends. The alkaline earth oxides tend to have high vapor pressures. Zirconia, yttria, and hafnia have quite low vapor pressures; however, at 1925 °C (3500 °F) only hafnia meets the recession rate criterion. There are few data for complex oxides, which likely exhibit vaporization with one component more volatile than another. An example of this is $BaZrO_3$, where BaO is the primary vapor species. In figure 5 it was assumed that $CaZrO_3$ and $SrZrO_3$ vaporize similarly so that some vapor pressures could be estimated. Data for the carbides, borides, and nitrides (figs. 6 and 7 and table I) are derived from measurements made under vacuum. The presence of an oxygen atmosphere rapidly oxidizes these materials, as will

be discussed. Nonetheless, nonoxides with high vapor pressures are not suitable as ultra-high-temperature materials. In general, the carbides tend to have lower vapor pressures than the borides or nitrides although Al_4C_3 and SiC are exceptions. The nitrides have higher vapor pressures because they decompose to nitrogen, although the vapor pressures of HfN and ZrN are rather low. Few data could be found for the borides, but ZrB_2 does have a low vapor pressure. Again, the interaction of these materials with oxygen must be considered.

Oxidation

The oxidation behavior of materials is crucial for their usefulness in an oxidizing environment at the high temperatures examined in this study. The oxidation characteristics of numerous high-melting-point materials reported in the literature were investigated. Surface recession rates (the rate of conversion of the base material to a solid oxide) after isothermal oxidation for 1 and 100 hr were calculated for several categories of materials. Many assumptions were made in calculating the recession rates. Often the oxidation tests from which data were obtained were conducted for relatively short times (e.g., less than 10 hr). It was assumed that the oxidation rates measured at short times were valid to 100 hr. Similarly the reaction products and surface scales observed after short exposure were assumed to be identical to those that would be present after longer exposure. We often found oxidation rates calculated and reported that were based on simple weight change measured during high-temperature exposure. Numerous materials, such as the nitrides and the carbides, are known to evolve gaseous reaction products, and in these cases we corrected the weight change according to the reported or most probable reaction to account for the evolved gas. For example, the oxidation of silicon nitride can be described by the reaction

$$Si_3N_4 + 3O_2 = 3SiO_2 + 2N_2(g)$$

For this system the weight change measured during oxidation is a combination of a weight increase due to oxygen pickup and a weight decrease due to nitrogen evolution. Similar corrections must be made for carbides to account for carbon monoxide evolution. In some instances researchers were able to measure actual amounts of oxygen consumed during oxidation (e.g., refs. 24 and 25), and in such cases no corrections were necessary. Recession rates were calculated on the assumption that the material tested had the reported theoretical density (refs. 4 to 7). Many researchers actually reported less than full density for the materials they studied, but we did not take this into consideration. In general, we made no attempt to critically evaluate reported data.

Results for each of the material categories are summarized in figures 8 and 9. The materials examined within each category, the reported or assumed oxidation reaction and pertinent references are presented in table II. The data for Si_3N_4 and SiC were put in a special category designated "silica formers" because these materials exhibited drastically different recession rates from those of other nitrides and carbides. Oxidation kinetics for most materials followed a parabolic rate relationship. Several carbides were reported to follow a linear oxidation rate as a result of scale cracking and spallation at elevated temperatures. For materials following a parabolic rate, the difference between the surface recession after 1 and 100 hr is simply a factor of 10, as can be seen from the figures. However, the difference

in recession for materials obeying linear kinetics is a factor of 100. This accounts for the relative upward shift in the position of the carbides.

Difficulties often arise when comparing the oxidation rates for the same materials when measured and reported by different investigators. This is illustrated in the oxidation results reported for $MoSi_2$. One reported rate (ref. 24) was three to four orders of magnitude greater than that reported by other researchers (ref. 26). This difference probably resulted from the fact that the rates reported in reference 24 apply to measurements made before the formation of a silica scale. The lower rates reported in reference 26 are similar to other reported rates for silica formers (refs. 27 to 32). Several studies presented anomalous oxidation rates that could not be resolved with other data. The oxidation rates for $TiSi_2$ and WSi_2 (refs. 25, 26, 33, and 34) appeared unusually high for the formation of a silica scale and may also have been measured before the formation of a continuous silica scale. These data are shown in table II but not included in figures 9 and 10. As expected, the lowest surface recession rates are associated with materials that are currently being used for oxidation protection, namely, alumina and silica formers. In aeroturbine engines a conservative recession rate for hot-section components such as turbine blades is assumed to be 0.25 μm/hr. Furthermore it is assumed that the recession rate is linear in time. This latter assumption is considered reasonable for a component undergoing thermal cycling, where scale cracking and spallation are expected to prevail. Taking the assumed maximum allowable recession rate permitted us to evaluate each material examined in this study for high-temperature usefulness. Dashed lines indicating the acceptable amount of recession after 1 and 100 hr are shown in figures 8 and 9. In the temperature range of interest (1650 to 2200 °C; 3000 to 4000 °F) all materials, with the exception of the silica formers, exhibited unacceptably high amounts of recession. For reasons previously stated, thermochemical considerations disqualify silicon-based systems from use in this temperature range. Several comments should be emphasized at this point. First, the data for each material category shown in the figures are for isothermal oxidation. As noted earlier, thermal cycling always results in accelerated recession rates because of scale cracking and spallation (ref. 35). Consequently surface recession in a turbine engine environment will be greater than that shown in figures 8 and 9. Second, the oxides SiO_2 and B_2O_3 are noncrystalline and viscous liquids above certain temperatures. Thus they might not be expected to remain on the surface of a component in a high-velocity gas flow characteristic of turbine engines. Centrifugal forces on rotating components may also cause loss of a viscous scale. Furthermore at the temperatures of interest certain scales may simply melt and thus be of little value (e.g., Al_2O_3 melts at 2045 °C (3713 °F)). A final, but certainly not trivial, concern is the volatility of protective scales. It has been established that certain oxide scales that are protective in static environments become nonprotective in dynamic environments (e.g., Cr_2O_3 scales, ref. 36).

In summary, figures 8 and 9 show conservative results from which we concluded that no nonoxide material has sufficient surface stability to be generally useful throughout the temperature range from 1650 to 2200 °C (3000 to 4000 °F).

EVALUATION OF OXIDES

On the basis of the analysis a large number of oxide ceramics (appendix B) were initially suggested as possible components of an oxide-containing composite system. (There are, of course, many other oxides, including those containing several different metal atoms, but property data for them are nearly nonexistent.)

Materials that were clearly unsuitable for use above 1650 °C (3000 °F) were then eliminated from further consideration (appendix B). As discussed earlier, the properties of primary interest in evaluating mechanical or microstructural stability above 1650 °C (3000 °F) are, first, the absence of phase transformations at or below potential use temperatures and, second, such properties as creep rate and grain growth rate at the highest use temperatures. Thus, for evaluating the long-term structural capabilities of the oxides that pass the environmental stability tests, it becomes necessary to examine the literature for phase and defect data that can be used to evaluate resistance to microstructural change.

Applying the phase stability criteria to the oxides listed in appendix B, we first eliminated from consideration those materials with melting temperatures that are too low. Melting temperatures are listed in many sources (refs. 9 and 37 to 43 as well as the Wright-Patterson Program Review and unpublished data taken by Cerac, Inc., of Milwaukee, Wisconsin), but the values given for any one material vary by as much as 300 deg C. This variation is due to several factors, including the difficulty of accurately measuring such high temperatures and the inability to obtain very high-purity materials. When such a range of temperatures was found, either the most common value or a value from midrange was selected. We found similar variation in other property data. These data must be determined more accurately as part of a materials evaluation program. Other oxides may also be eliminated because of various types of solid-state phase transformations.

Turning next to diffusion-related properties, a literature search for the remaining oxides revealed that in all cases creep or grain-growth data are either absent or subject to erroneous interpretation because impurity oxide phases or nonstoichiometric conditions were present in the material specimens. In both cases defect-controlled processes can occur at a lower temperature or at a significantly greater rate than in a pure stoichiometric material. In addition, essentially all the available literature data were obtained on polycrystalline specimens, in which grain-boundary diffusion rather than bulk lattice diffusion is probably the overwhelming source of time-dependent microstructural change. Thus we judged the current status of defect-controlled property data for high-temperature oxides to be inconclusive regarding quantitative or even qualitative evaluation of their mechanical stability.

Other physical and mechanical properties related to the structural performance of the remaining oxide ceramics are their thermal expansion characteristics, such as total expansion and expansion coefficient, and their specific stiffness. For some materials these properties are obtainable from the literature and are indicated in the appendix A. However, these properties are secondary to the defect-controlled properties and therefore cannot at present serve to focus the search for an oxide material with high potential for structural use above 1650 °C (3000 °F).

The oxides that remain possible candidates for composite systems to be used above 1650 °C (3000 °F) as follows: $CaO \cdot HfO_2$, $CaZrO_3$, $HfO_2(+Y_2O_3)$, $3MgO \cdot Y_2O_3$, $MgO \cdot ZrO_2$, $NiAl_2O_4$, $SrZrO_3$, $SrZr_2O_4$, Y_4GeO_8, $ZrO_2(+Y_2O_3)$, Sc_2O_3, Y_2O_3, and the rare earth oxides (e.g., Pr_2O_3 and $SrYb_2O_4$).

A PROPOSED PROGRAM

At this point the task at hand is to generate a research and development program that will take us from the selection of these few candidates to the identification and ultimate demonstration of ceramic composite systems as specific engine components. A proposed program to span this gap from fundamental materials science to component development is shown in figure 10. The absolute timeframe for accomplishing this program is not shown because it is greatly dependent on available resources.

The three phases of the program are

(I) Material studies
(II) Composite materials development and verification
(III) Component development

Each phase of the program is discussed here, but first some caveats are in order.

The program as outlined here assumes success. That is, no iterative loops are shown in the layout although in reality many such loops will be required as unforeseen obstacles are met. Also, substudies, which surely will be necessary, are not shown. For example, during phase II (composite material development and verification) attention must be directed to characterizing and improving fibers and fiber surfaces. Also, fiber/matrix interface characterization will have to be addressed under verification of thermal stability in phase II. Although these necessary substudies are not shown in figure 10, they will be addressed as more detailed plans are generated for each phase of the program. At this point only an overview of the program is presented in order to display the starting point, the end point, and the logical steps to get from start to end.

Phase I - Material Studies

Phase I is intended to take us from a selection of potential materials based on the literature and past experience to a selection of composite systems (fiber material and matrix material) based on experimental evaluation of key properties.

Three efforts will be pursued in parallel during the initial portion of phase I. First, a more detailed literature search will be conducted of the candidate materials (table III). Second, efforts will be made to personally communicate with selected key authors relevant to each material. Such contacts can be extremely helpful in learning nuances of materials and evaluation techniques that often are not included in journal articles. Third, procurement of materials will be started. Materials will be procured in whatever forms are readily available. No fibers of the candidate materials are expected to be available at this stage.

Cursory and general evaluations will be conducted as materials are received. Evaluations will depend somewhat on the form in which a given material is available. Generally, it is anticipated that such properties as density, purity, X-ray phase identification, melting point decomposition temperature, and sinterability will be determined.

At point A worthy materials will be selected for continued study. Selected materials will be subjected to detailed studies in three areas: thermodynamic stability, surface stability, and mechanical stability.

Thermodynamic stability will involve primarily vaporization and phase stability studies. Vapor species and pressures as well as phase stability will be determined or verified.

Surface stability studies will be conducted in static and flowing oxidizing environments under both isothermal and cyclic exposure conditions. Weight changes and recession rates will be measured and surface phases identified. Both oxygen partial pressure and flow rate are expected to effect surface stability.

Mechanical stability will be judged by observing defect-controlled properties such as sinterability, grain growth, and creep, where possible, as a function of time-and-temperature exposures to combustion gases. Thermal shock resistance, a potentially major problem with oxides, will be evaluated and residual strength measured as a function of number of cycles and temperature of exposure.

At decision point B specific materials will be identified as candidates for fibers and as candidates for matrices. At this point specific material combinations, fiber candidate and matrix candidate, will be selected for compatibility studies. Up to this point all candidates will have been evaluated as individual materials. Bulk material couples will be subjected to appropriate time, temperature, and atmosphere combinations, and any interfacial instabilities will be noted.

Point C is a major decision point at which specific composite systems (fiber/matrix combination) will be selected for development in phase II.

Phase II - Composite Materials Development and Verification

Fiber synthesis and composite fabrication will be pursued in parallel efforts. It is anticipated that these efforts will be primarily contracted to industry. Once fiber and composite approaches are available (point D in fig. 10), studies will be started to verify that the composite systems (fiber/matrix combinations) are indeed thermally stable. At the same time the mechanical behavior of the composite systems will be documented. As soon as a composite system is found to be thermally stable and have adequate mechanical properties, it will be evaluated under simulated mission conditions. This will test the composite at combinations of time, temperature, stress, oxygen pressure, gas velocity, etc., that simulate a proposed mission for the advanced engine. At point E, the completion of phase II, the most promising composite systems will be chosen for continued development as components.

Phase III - Component Development

At this point a complete profile of thermal and mechanical behavior will be available for each composite system that has survived phase II. This information will then be compared with the design requirements of some specific engine components. The most promising composite system will be chosen for each of several engine components; then manufacturing studies will commence for each composite/component combination. Likely components that will benefit most from ceramic composite capabilities are turbine blades, vanes, shrouds, combustors, and exhaust nozzles. As prototype components become available, they will be evaluated by mission simulation testing.

At point F some successful composite/component combinations should be identified that can be made immediately available to the engine industry. It is also quite likely that some composite/component combinations with shortcomings will be identified. Depending on the specific problems identified, these systems will be iterated back through the appropriate portions of the program.

CONCLUSIONS

The program outlined in this report is believed to be a logical and orderly approach to evaluating ceramic matrix composites for engine components. It covers the required basic materials science early in the program. It also reflects a realization that advanced high-temperature materials cannot be developed without due attention to the final application. Thus design and manufacturing requirements are an integral part of the program.

The three phases of the proposed program identify three major work areas: materials science, composite development, and component design and manufacture. Major efforts are required in each of these three areas if ceramic matrix composites are to reach full fruition as advanced engine components. Specific planning is now required in each area so that each program phase may be successfully executed in relevant NASA programs.

Material	Melting temperature,[a] T_m, °C	Material density,[a] ρ, g/cm^3	Young's modulus,[b] GPa		E/ρ_{RT}	$E/\rho_{1100°C}$
			E_{RT}	$E_{1100°C}$		
Al_2O_3	2045	3.98	443	415	111.3×10^6	104.3×10^6
BaO	1920	5.72	---	---	---	---
BeO	2550	3.01	400	352	132.9×10^6	116.9×10^6
CaO	2610	3.32	---	---	---	---
CeO_2	2600	7.28	169	98	23.2×10^6	13.5×10^6
Cr_2O_3	2266	5.21	---	---	---	---
HfO_2	2758	9.68	---	---	---	---
La_2O_3	2300	6.57	---	---	---	---
MgO	2800	3.58	387	323	108.1×10^6	90.2×10^6
Pr_2O_3	2200	6.32	---	---	---	---
Sc_2O_3	2300	3.84	225	---	58.6×10^6	---
SiO_2	1725	2.32	74	82	31.9×10^6	35.3×10^6
SrO	2420	4.70	---	---	---	---
Ta_2O_5	1872	8.02	---	---	---	---
ThO_2	3220	10.00	253	204	25.3×10^6	20.4×10^6
TiO_2	1850	4.25	288	---	67.8×10^6	---
UO_2	2850	10.96	204	183	18.6×10^6	16.7×10^6
Y_2O_3	2410	5.03	169	---	33.6×10^6	---
ZrO_2	2700	5.56	253	148	45.5×10^6	26.6×10^6
$BaO \cdot ZrO_2$	2647	6.26	---	---	---	---
$CaO \cdot HfO_2$	2470	6.05	---	---	---	---
$2CaO \cdot SiO_2$	2130	3.28	---	---	---	---
$CaZrO_3$	2327	4.76	---	---	---	---
$HfO_2(Y_2O_3)$	2400	9.70	---	---	---	---
$LaCrO_3$	2510	----	---	---	---	---
$MgO \cdot Al_2O_3$	1995	3.59	239	190	66.6×10^6	52.9×10^6

[a]References 9 and 37 to 43 as well as Wright-Patterson Program Review and unpublished data taken by Cerac, Inc., of Milwaukee, Wisconsin.
[b]References 4 to 7.
[c]Reference 44.
[d]Reference 45.
[e]References 11 to 23.

PRECEDING PAGE BLANK NOT FILMED

A

PROPERTY DATA

Thermal expansion coefficient,[c] μm/K		Thermal diffusivity,[d] k_{1300K}, W/cm K	Crystal structure	Vapor flux at 2200 K,[e] g/cm^2 hr	Comments
α_{293K}	α_{1300K}				
5.4	9.9	0.055	Cubic	--------	T_m < 2000 °C
-----	-----	-----	----------	--------	T_m < 2000 °C
6.3	11.6	-----	----------	--------	----------
11.2	14.7	-----	Cubic	--------	----------
9.5	14.1	-----	Orthorhombic	--------	T_m < 2000 °C
8.8	7.6	-----	----------	--------	T_m < 2000 °C
3.8	9.7	-----	Cubic	$4.8x10^{-4}$	----------
10.8	-----	-----	----------	--------	----------
10.2	15.7	-----	----------	--------	----------
7.8	9.2	-----	Cubic	--------	----------
6.6	11.3	-----	Cubic	--------	Phase stability
-----	-----	-----	Hexagonal	--------	----------
1.14	1.14	-----	Perovskite	--------	----------
-----	-----	-----	Cubic solid solution	--------	----------
7.7	10.6	-----	Cubic solid solution	--------	----------
-----	-----	-----	Ca ferrite	--------	----------
-----	-----	-----	----------	--------	----------
7.3	9.2	-----	Rhombohedral	$5x10^{3}$	----------
8.8	10.5	-----	Cubic	$3x10^{-4}$	----------
-----	-----	0.35	Cubic	$5x10^{-6}$	----------
-----	-----	-----	Tetragonal	--------	----------
-----	-----	-----	Hexagonal	$9x10^{-1}$	----------
7.9	13.9	0.24	Cubic	$5x10^{-6}$	----------
-----	-----	-----	Cubic	$3x10^{-4}$	----------
-----	-----	0.35	Cubic	$3x10^{-7}$	----------
7.0	10.6	0.061	Hexagonal	$4.1x10^{-3}$	Moderately high vapor pressure

Material	Melting temperature,[a] T_m, °C	Material density,[a] ρ, g/cm^3	Young's modulus,[b] GPa		E/ρ_{RT}	E/$\rho_{1100°C}$
			E_{RT}	$E_{1100°C}$		
$MgO \cdot SiO_2$	1890	-----	---	---	---------	---------
$MgO \cdot ZrO_2$	2110	-----	---	---	---------	---------
$NiAl_2O_4$	2020	4.45	84	---	18.9×10^6	---------
$2SiO_2 \cdot 3Al_2O_3$	1850	3.20	148	---	46.3×10^6	---------
$SrO \cdot Al_2O_3$	1900	-----	---	---	---------	---------
$SrZrO_3$	2650	5.48	84	---	15.3×10^6	---------
Sr_2ZrO_4	2200	-----	---	---	---------	---------
Y_4GeO_8	2000	-----	---	---	---------	---------
$ZrO_2(Y_2O_3)$	2805	5.70	295	---	51.8×10^6	---------
Yb_2O_3	2400	9.25	190	---	20.5×10^6	---------
$Ba_3Yb_4O_9$	2200	-----	---	---	---------	---------
$YbCrO_3$	2335	-----	---	---	---------	---------
$Yb_2O_3(ThO_2)$	2400	-----	---	---	---------	---------
$Yb_2O_3(Nd_2O_3)$	2400	-----	---	---	---------	---------
$SrYb_2O_4$	2200	-----	---	---	---------	---------
C	3652	-----	---	---	---------	---------
Al_4C_3	2100	2.99	---	---	---------	---------
HfC	3890	12.67	324	296	25.6×10^6	23.4×10^6
NbC	3480	7.82	455	379	58.2×10^6	48.5×10^6
PrC_2	2535	5.73	---	---	---------	---------
SiC	2827	3.21	414	379	129.0×10^6	118.1×10^6
TaC	3880	14.50	510	462	35.2×10^6	31.9×10^6
TiC	3140	4.92	448	---	91.1×10^6	---------
ZrC	3420	6.56	386	365	58.8×10^6	55.6×10^6
AlN	2570	3.26	345	310	105.8×10^6	95.1×10^6
BN	2500	2.28	69	---	30.3×10^6	---------
HfN	3300	13.94	---	---	---------	---------
Si_3N_4	1900	3.18	296	276	93.1×10^6	86.8×10^6
TaN	3087	14.36	---	---	---------	---------

[a]References 9 and 37 to 43 as well as Wright-Patterson Program Review and unpublished data taken by Cerac, Inc., of Milwaukee, Wisconsin.
[b]References 4 to 7.
[c]Reference 44.
[d]Reference 45.
[e]References 11 to 23.

Thermal expansion coefficient,[c] μm/K		Thermal diffusivity,[d] k_{1300K}, W/cm K	Crystal structure	Vapor flux at 2200 K,[e] g/cm^2 hr	Comments
α_{293K}	α_{1300K}				
----	----	-----	Cubic	--------	T_m < 2000 °C
----	----	0.283	----------	--------	Toxic
----	----	-----	Cubic	6.5×10^{-2}	Reacts with water
----	----	0.017	Cubic	28	High vapor pressure
----	----	-----	Hexagonal	--------	High vapor pressure
0.75	1.21	0.057	Monoclinic	2.1×10^{-5}	Phase changes
----	----	-----	Hexagonal	2.2×10^{-2}	High vapor pressure
----	----	0.072	Cubic	0.61	High vapor pressure
----	----	-----	Cubic	--------	----------
----	----	-----	Cubic	--------	----------
----	----	-----	Tetragonal	--------	Phase stability; T_m < 2000 °C
----	----	-----	Cubic	16	High vapor pressure
----	----	-----	Orthorhombic	--------	T_m < 2000 °C
----	----	0.029	Cubic	--------	Toxic
----	----	0.032	Tetragonal	--------	T_m < 2000 °C
----	----	-----	Cubic	--------	Toxic
----	----	0.27	Cubic	1.7×10^{-4}	----------
4.9	7.2	-----	Monoclinic	4.5×10^{-4}	Phase stability
5.7	7.8	-----	Cubic	0.40	----------
----	----	-----	Orthorhombic	--------	----------
3.3	5.8	-----	Monoclinic	--------	Phase stability
5.6	7.3	-----	Monoclinic	9.6×10^{-4}	----------
6.4	8.9	-----	Cubic solid solution	--------	----------
4.0	8.3	-----	----------	--------	High vapor pressure
----	----	-----	Hexagonal	2×10^{3}	----------
1.8	7.1	0.25	Hexagonal	60	----------
----	----	0.14	Cubic	1×10^{-2}	----------
0.8	3.7	0.06	Hexagonal	1×10^{4}	----------
----	----	-----	Hexagonal	5	----------

Material	Melting temperature,[a] T_m, °C	Material density,[a] ρ, g/cm^3	Young's modulus,[b] GPa		E/ρ_{RT}	$E/\rho_{1100°C}$
			E_{RT}	$E_{1100°C}$		
TiN	2950	5.44	600	---	110.3×10^6	---
HfB_2	3250	11.20	---	---	---	---
TaB_2	3100	12.60	248	---	19.7×10^6	---
TiB_2	2980	4.52	496	---	109.7×10^6	---
ZrB_2	3050	6.09	496	---	81.4×10^6	---
$MoSi_2$	2030	6.26	379	276	60.5×10^6	44.1×10^6
WSi_2	2165	9.87	448	262	45.4×10^6	26.5×10^6
$BaZrO_3$	----	-----	---	---	---	---

[a]References 9 and 37 to 43 as well as Wright-Patterson Program Review and unpublished data taken by Cerac, Inc., of Milwaukee, Wisconsin.
[b]References 4 to 7.
[c]Reference 44.
[d]Reference 45.
[e]References 11 to 23.

Thermal expansion coefficient,[c] μm/K		Thermal diffusivity,[d] k_{1300K}, W/cm K	Crystal structure	Vapor flux at 2200 K,[e] g/cm^2 hr	Comments
α_{293K}	α_{1300K}				
6.3	10.4	----	Cubic	1	----------
---	----	----	Hexagonal	------	----------
---	----	----	Hexagonal	------	----------
---	----	----	Hexagonal	$1x10^{2}$	----------
---	----	----	Hexagonal	$1x10^{-3}$	----------
6.8	9.6	----	Tetragonal	------	----------
7.2	9.7	----	Tetragonal	------	----------
---	----	----	----------	0.23	----------

APPENDIX B

OXIDES CONSIDERED AS POSSIBLE COMPONENTS OF OXIDE-CONTAINING COMPOSITE SYSTEMS

Oxides initially suggested:

Al_2O_3	ZrO_2	$3MgO \cdot Y_2O_3$	Y_4GeO_8
BaO	Sc_2O_3	$BaO \cdot ZrO_2$	$MgO \cdot ZrO_2$
BeO	SiO_2	$CaO \cdot HfO_2$	$NiAl_2O_4$
CaO	SrO	$2CaO \cdot SiO_2$	$2SiO_2 \cdot 3Al_2O_3$
Ta_2O_5	$CaZrO_3$	$SrO \cdot Al_2O_3$	$ZrO_2(+Y_2O_3)$
Cr_2O_3	ThO_3	$HfO_2(+Y_2O_3)$	$SrZrO_3$
HfO_2	TiO_2	$LaCrO_3$	Sr_2ZrO_4
La_2O_3	UO_2	$MgO \cdot Al_2O_3$	$MgO \cdot SiO_2$
MgO	Y_2O_3		

and the rare earth oxides (e.g., Pr_2O_3, $YbCrO_3$, and CeO_2).

Oxides eliminated from consideration for use above 1650 °C (3000 °F):

(1) Melting temperature below 2000 °C (3600 °F)

BaO	Ta_2O_5	$Mgo \cdot Al_2O_3$	$Sr \cdot Al_2O_3$
SiO_2	TiO_2	$2SiO_2 \cdot 3Al_2O_3$	

(2) Toxic or radioactive

BeO	ThO_2	UO_2	$Yb_2O_3(+ThO_2)$

(3) Vapor pressure too high

Al_2O_3	Cr_2O_3	MgO	$LaCrO_3$
CaO	La_2O_3	SrO	$BaO \cdot ZrO_2$
CeO_2			

(4) Phase instability

CaO	ZrO_2	$MgO \cdot SiO_2$	
HfO_2	Yb_2O_3	$2CaO \cdot SiO_2$	

REFERENCES

1. Fleischer, R.L.: High-Temperature, High-Strength Materials - An Overview. J. Met., vol. 37, no. 12, Dec. 1985, pp. 16-20.

2. Hillig, W.B.: Prospects for Ultra-High-Temperature Ceramic Composites. Tailoring Multiphase and Composite Ceramics, R.E. Tressler, et al., eds., Plenum, 1986, pp. 697-712.

3. Morrell, R.: Handbook of Properties of Technical and Engineering Ceramics. Her Majesty's Stationery Office, London, 1985.

4. Lynch, J.F.; Ruderer, C.G.; and Duckworth, W.H.: Engineering Properties of Selected Ceramic Materials. American Ceramic Society, 1966.

5. Engineering Property Data on Selected Ceramics, Vol. 3: Single Oxides. Metals and Ceramics Information Center, Battelle Columbus Laboratories, Report MCIC-HB-07-Vol. III, July 1981. (Avail. NTIS, AD-A104538.)

6. Engineering Property Data on Selected Ceramics, Vol. 2: Carbides. Metals and Ceramics Information Center, Battelle Columbus Laboratories, Report MCIC-HB-07-Vol. II, Aug. 1979. (Avail. NTIS, AD-A087519.)

7. Engineering Property Data on Selected Ceramics, Vol. 1: Nitrides. Metals and Ceramics Information Center, Battelle Columbus Laboratories, Report MCIC-HB-07-Vol. I, Mar. 1976 (Avail. NTIS, AD-A023773.)

8. Alper, A.M.: High Temperature Oxides. Academic Press, 1970.

9. Shaffer, P.T.B.: Materials Index. Plenum Press, 1964.

10. Bhatt, R.T.: Mechanical Properties of SiC Fiber-Reinforced Reaction Bonded Si_3N_4 Composites. NASA TM-87085, 1985.

11. Lowell, C.E.; and Sanders, W.A.: Mach 1 Oxidation of Thoriated Nickel Chromium at 1204 °C (2200 °F). Oxid. Met., vol. 5, no. 3, Dec. 1972, pp. 221-239.

12. Stearns, C.A.; Kohl, F.J.; and Fryburg, G.C.: Oxidative Vaporization Kinetics of Chromium (III) Oxide in Oxygen from 1270 to 1570 K. NASA TN D-7628, 1974.

13. Stull, D.R.; and Prophet, J.H.: JANAF Thermochemical Tables, U.S. National Bureau of Standards, Washington, D.C., 1971.

14. Chase, M.W., et al.: JANAF Thermochemical Tables, 1974 Supplement. J. Phys. Chem. Ref. Data, vol. 3, no. 2, 1974, pp. 311-480.

15. Chase, M.W., et al.: JANAF Thermochemical Tables, 1975 Supplement. J. Phys. Chem. Ref. Data, vol. 4, no. 1, 1975, pp. 1-175.

16. Chase, M.W., et al.: JANAF Thermochemical Tables, 1978 Supplement. J. Phys. Chem. Ref. Data, vol. 7, no. 3, 1978, pp. 793-940.

17. Barin, I.; and Knacke, O.: Thermomechanical Properties of Inorganic Substances, Springer-Verlag, 1973.

18. Barin, I.; Knacke, O.; and Kubaschewski, O.: Thermochemical Properties of Inorganic Substances, Supplement, Springer-Verlag, 1977.

19. Chandrasekharaiah, M.S.: Volatilities of Refractory Inorganic Compounds. The Characterization of High Temperature Vapors, J.L. Margrave, ed., John Wiley & Sons, 1967, pp. 495-507.

20. Ackermann, R.J.; and Thorn, R.J.: Vaporization of Oxides. Progress in Ceramic Science, Vol. 1, J.E. Burke, ed., Pergammon Press, 1961, pp. 39-88.

21. Ackerman, R.J.; and Rauh, E.G.: A High-Temperature Study of the Stoichiometry, Phase Behavior, Vaporization Characteristics, and Thermodynamic Properties of the Cerium + Oxygen System. J. Chem. Thermodynamics, vol. 3, no. 5, Sept. 1971, pp. 609-624.

22. Odoj, R.; and Hilpert, K.: Massenspektrometrische Hochtemperature Messung des Systems BaO-ZrO_2 amd Bestimmung Thermodynamischer Daten des $BaZrO_3$. (Mass Spectrometric High Temperature Measurements of the Barium Oxide - Zirconium Dioxide System and the Determination of Thermodynamic Data for Barium Zirconate. Clarification of the Counter-Stopping Capacity of Coated Particles for Solid Fission Products by Zirconium Dioxide Addition.) Ber. Kernforschungsanlage Juelich, 1975.

23. Searcy, A.M.: The Reactions of High Temperature Materials. Chemical and Mechanical Behavior of Inorganic Materials, A.W. Searcy, D.V. Ragone, and U. Columbo, eds., Wiley Interscience, 1970, pp. 57-80.

24. Chang, Y.A.: Oxidation of Molybdenum Disilicide. J. Mater. Sci., vol. 4, no. 7, July 1969, pp. 641-643.

25. Berkowitz-Mattuck, J.B.: Mechanisms of Oxidation of Ta-10W Alloy Coated With Tungsten Disilicide. J. Electrochem. Soc., vol. 116, no. 5, May 1969, pp. 700-709.

26. Schlichting, J.: High Temperature Oxidation of Disilicides in the System $MoSi_2$-$TiSi_2$. Ceramurgie Int., vol. 4. no. 4, Oct.-Dec. 1978, pp. 162-166.

27. Costello, J.A.; and Tressler, R.E.: Oxidation Kinetics of Silicon Carbide Crystals and Ceramics: I. In Dry Oxygen. J. Am. Ceram. Soc., vol. 69, no. 9, Sept. 1986, pp. 674-681.

28. Hinze, J.W.; Tripp, W.C.; and Graham, H.C.: The High-Temperature Oxidation of Hot-Pressed Silicon Carbide. Mass Transport Phenomena in Ceramics, A.R. Cooper and A.H. Heuer, eds., Plenum, 1975, pp. 409-420.

29. Singhal, S.C.: Oxidation Kinetics of Hot-Pressed Silicon Carbide. J. Mater. Sci., vol. 11, no. 7, July 1976, pp. 1246-1253.

30. Hirai, T.; Niihara, K.; and Goto, T.: Oxidation of CVD Si_3N_4 at 1550° to 1650 °C," J. Am. Ceram. Soc., vol. 63, no. 7-8, July-Aug. 1980, pp. 419-424.

31. Rosolowski, J.H.; and Greskovich, C.D.: Ceramic Sintering. SRD-74-116, General Electric Co., Oct. 1974. (Avail. NTIS, AD-A001012.)

32. Franz, I.; and Langheinrich, W.: Conversion of Silicon Nitride Into Silicon Dioxide Through the Influence of Oxygen. Solid-State Electron., vol. 14, no. 5, June 1971, pp. 499-505.

33. Samsonov, G.V.; Lavrenko, V.A.; and Glebov, L.A.: Oxidation of Tungsten Disilicide in Oxygen. Sov. Powder Metall. Met. Ceram. (Engl. Transl.), vol. 13, no. 3, Mar. 1974, pp. 232-235.

34. Pugach, E.A.; Golovka, E.I.; and Dvorina, I.V.: High-Temperature Oxidation of TiB_2-$TiSi_2$ Alloys. Sov. Powder Metall. Met. Ceram. (Engl. Trans.), vol. 16, no. 2, Feb. 1977, pp. 108-111.

35. Barrett, C.A.; and Lowell, C.E.: Comparison of Isothermal and Cyclic Oxidation Behavior of Twenty-Five Commercial Sheet Alloys at 1150 °C. Oxid. Met., vol. 9, no. 4, Aug. 1975, pp. 307-355.

36. Barrett, C.A.; Johnston, J.R.; and Sanders, W.A.: Static and Dynamic Cyclic Oxidation of 12 Nickel-, Cobalt-, and Iron-Base High-Temperature Alloys. Oxid. Met., vol. 12, no. 4, Aug. 1978, pp. 343-377.

37. Weast, R.C., ed.: CRC Handbook of Chemistry and Physics, 67th ed., CRC Press, Boca Raton, FL, 1986.

38. Levin, E.M.; Robbins, C.R.; McMurdie, H.F.: Phase Diagrams for Ceramists, American Ceramic Society, Columbus, OH, 1964.

39. Levin, E.M.; Robbins, C.R.; McMurdie, H.F.: Phase Diagrams for Ceramists, Vol. 2, 1969 Supplement, American Ceramic Society, Columbus, OH, 1969.

40. Levin, E.M.; and McMurdie, H.F.: Phase Diagrams for Ceramists, Vol. 3, 1975 Supplement, American Ceramic Society, Columbus, OH, 1975.

41. Roth, R.S.; Negas, T.; and Cook, L.P.: Phase Diagrams for Ceramists, Vol. 4, American Ceramic Society, Columbus, OH, 1981.

42. Roth, R.S.; Negas, T.; and Cook, L.P.: Phase Diagrams for Ceramists, Vol. 5, American Ceramic Society, Columbus, OH, 1983.

43. Samsonov, G.V.: Plenum Press Handbooks of High-Temperature Materials, No. 2 - Properties Index, 1964.

44. Touloukian, Y.S., et al., eds.: Thermophysical Porperties of Matter, vol. 13, Thermal Expansion, Nonmetallic Solids, IFI/Plenum, 1970.

45. Touloukian, Y.S., et al., eds.: Thermophysical Properties of Matter, vol. 2, Thermal Conductivity, Nonmetallic Solids, IFI/Plenum, 1970.

46. Hindam, H.; and Whittle, D.P.: Microstructure, Adhesion and Growth Kinetics of Protective Scales on Metals and Alloys. Oxid. Met., vol. 18, nos. 5/6, Dec. 1982, pp. 245-284.

47. Lavrenko, V.A., et al.: High-Temperature Oxidation of Titanium Carbide in Oxygen. Oxid. Met., vol. 9, no. 2, Apr. 1975, pp. 171-180.

48. Voitovich, R.R.; and Pugach, E.A.: High-Temperature Oxidation of Titanium Carbide. Sov. Powder Metall. and Met. Ceram. (Engl. Trans.), vol. 11, no. 2, Feb. 1972, pp. 132-136.

49. Voitovich, R.F.; and Pugach, E.A.: High-Temperature Oxidation of ZrC and HfC. Sov. Powder Metall. and Met. Ceram. (Engl. Trans.), vol. 12, no. 11, Nov. 1973, pp. 916-921.

50. Kuriakose, A.K.; and Margrave, J.L.: The Oxidation Kinetics of Zirconium Diboride and Zirconium Carbide at High Temperatures. J. Electrochem. Soc., vol. 111, no. 7, July 1964, pp. 827-831.

51. Lavrenko, V.A., et al.: Kinetics of High-Temperature Oxidation of Boron Carbide in Oxygen. Oxid. Met., vol. 10, no. 2, Apr. 1976, pp. 85-95.

52. Shevchenko, A.S., et al.: Oxidation of Zirconium and Niobium Carbides. Sov. Powder Metall. and Met. Ceram. (Engl. Transl.), vol. 19, no. 1, Jan. 1980, pp. 48-52.

53. Kang, S.G.; and Fromm, E.: Reactions of Molybdenum and Tungsten Carbides With Oxygen at High Temperatures. Metall. Trans. A, vol. 12, no. 12, Dec. 1981, pp. 1993-1998.

54. Voitovich, R.F.; and Pugach, E.A.: High-Temperature Oxidation Characteristics of the Carbides of the Group VI Transition Metals. Sov. Power Metall. and Met. Ceram. (Engl. Transl.), vol. 12, no. 4, Apr. 1973, pp. 314-318

55. McDonald, N.F.; and Ramsley, C.E.: The Oxidation of Hot-Pressed Titanium Carbide and Titanium Boride in the Temperature Range 300° - 1000 °C. Powder Metall. No. 3, 1959, pp. 172-176.

56. Voitovich, R.F.; and Pugach, E.A.: High-Temperature Oxidation of Borides of the Group IV Metals. I. Oxidation of Titanium Diboride. Sov. Powder Metall. and Met. Ceram. (Engl. Transl.), vol. 14, no. 2, Feb. 1975, pp. 132-135.

57. Tripp, W.C.; and Graham, H.C.: Thermogravimetric Study of the Oxidation of ZrB_2 in the Temperature Range of 800° to 1500 °C. J. Electrochem. Soc., vol. 118, no. 7, July 1971, pp. 1195-1199.

58. Voitovich, R.F.; Pugach, E.A.; and Mensikova, L.A.: High-Temperature Oxidation of Zirconium Diboride. Sov. Powder Metall. and Met. Ceram. (Engl. Trans.), vol. 6, no. 6, June 1967, pp. 462-465.

59. Kuzenkova, M.A.; and Kislyi, P.S.: The Oxidation Resistance of Alloys of Zirconium Boride With Molybdenum Disilicide. Sov. Powder Metall. and Met. Ceram. (Engl. Trans.), vol. 4, no. 10, Oct. 1965, pp. 841-844.

60. Kaufman, L.E.; Clougherty, V.; and Berkowitz-Mattuck, J.B.: Oxidation Characteristics of Hafnium and Zirconium Diboride. Trans. Metall. Soc. AIME, vol. 239, no. 4, Apr. 1967, pp. 458-466.

61. Voitovich, R.F.; and Pugach, E.A.: High-Temperature Oxidation of Borides of the Group IV Metals. II. Oxidation of Zirconium and Hafnium Diborides. Sov. Powder Metall. and Met. Ceram. (Engl. Trans.), vol. 14, no. 3, Mar. 1976, pp. 231-235.

62. Berkowitz-Mattuck, J.B.: High-Temperature Oxidation. III. Zirconium and Hafnium Diborides. J. Electrochem. Soc., vol. 113, no. 9, Sept. 1986, pp. 908-914.

63. Tripp, W.C.; Davis, H.H.; and Graham, H.C.: Effect of an SiC Addition on the Oxidation of ZrB_2. Am. Ceram. Soc. Bull., vol. 52, no. 8, Aug. 1973, pp. 612-616.

64. Basche, M.; and Schiff, D.: New Pyrolytic Boron Nitride. Mater. Des. Eng., vol. 59, no. 2, Feb. 1964, pp. 78-81.

65. Tsapuk, A.K.; Podobeda, L.G.; and Kovalevskii, N.N.: Oxidation of Materials Based on Boron Nitride. Sov. Powder Metall. and Met. Ceram. (Engl. Transl.), vol. 17, no. 3, Mar. 1978, pp. 208-210.

66. Voitovich, R.F.; and Pugach, E.A.: High-Temperature Oxidation of the Nitrides of the Groups IV and V Transition Metals. III. Oxidation of VN, NbN, and TaN. Sov. Powder Metall. and Met. Ceram. (Engl. Trans.), vol. 14, no. 12, Dec. 1975, pp. 1007-1010.

67. Voitovich, R.F.; and Pugach, E.A.: High-Temperature Oxidation of the Nitrides of the Group IV Transition Metals. II. Oxidation of Zirconium and Hafnium Nitrides. Sov. Powder Metall. and Met. Ceram. (Engl. Trans.), vol. 14, no. 9, Sept. 1975, pp. 747-750.

68. Suni, I., et al.: Thermal Oxidation of Reactively Sputtered Titanium Nitride and Hafnium Nitride Films. J. Electrochem. Soc., vol. 130, no. 5, May 1983, pp. 1210-1214.

69. Boch, P., et al.: Sintering, Oxidation and Mechanical Properties of Hot Pressed Aluminum Nitride. Ceram. Int., vol. 8, no. 1, Jan.-Feb. 1982, pp. 34-40.

TABLE I. - PRINCIPAL VAPOR SPECIES

Oxide	Principal vapor species	Carbide	Principal vapor species	Nitride	Principal vapor species
CeO_2	CeO_2,CeO	ZrC	Zr, C	TaN	N_2
SrO	SrO, Sr, O_2	TaC	C	TiN	Ti, N_2
MgO	Mg, O_2, MgO	NbC	C	HfN	N_2
CaO	Ca, O_2	HfC	Hf, C	ZrN	Zr, N_2
La_2O_3	La, O, O_2	TiC	Ti	BN	N_2
Al_2O_3	Al, O_2, Al_2O, AlO	SiC	Si, Si_2C, SiC_2	Si_3N_4	N_2
ZrO_2	ZrO_2	Al_4C_3	Al	AlN	Al, N_2
Y_2O_3	YO, O, O_2			ZrB_2	Zr, B
HfO_2	HfO_2			TiB_2	Ti, B
$BaZrO_3$	BaO				
$CaZrO_3$	CaO[a]				
$SrZrO_3$	SrO[a]				

[a]Predicted.

TABLE II. - OXIDATION CHARACTERISTICS OF MATERIALS

Category	Material	Reaction	Rate[a]	Reference	Comments
Silica formers	$MoSi_2$	$MoSi_2 + 2O_2 = Mo + 2SiO_2$	P	24,26	
	SiC	$2SiC + 3O_2 = 2SiO_2 + 2CO$		27-29	
	Si_3N_4	$Si_3N_4 + 3O_2 = SiO_2 + N_2$		30-32	
Alumina formers	Numerous metallic alloys	$4Al + 3O_2 = 2Al_2O_3$		46,(b)	Reference 46 presents compilation of 14 studies
Carbides	TiC	$2TiC + 3O_2 = 2TiO_2 + 2CO$	L	47,48	
	HfC	$2HfC + 3O_2 = 2HfO_2 + 2CO$		49	
	ZrC	$2ZrC + 3O_2 = 2ZrO_2 + 2CO$		50	
	B_4C	$B_4C + 4O_2 = 2B_2O_3 + CO_2$		51	Liquid product B_2O_3
	NbC	$4NbC + 7O_2 = 2Nb_2O_5 + 4CO_2$		52	
	Mo_2C	$2Mo_2C + 7O_2 = 4MoO_3 + CO_2$		53,54	Weight loss during oxidation
	W_2C	$2W_2C + 7O_2 = 4WO_3 + 2CO_2$		53,54	Weight loss during oxidation
Silicides	WSi_2	$2WSi_2 + 7O_2 = 2WO_3 + 2SiO_2$	P	25,33	
	$TiSi_2$	$TiSi_2 + 3O_2 = TiO_2 + 2SiO_2$		26,34	
Borides	TiB_2	$2TiB_2 + 5O_2 = 2TiO_2 + 2B_2O_3$		34,49,55,56	Liquid product B_2O_3
	ZrB_2	$2ZrB_2 + 5O_2 = 2ZrO_2 + 2B_2O_3$		48,57-63	Liquid product B_2O_3
	HfB_2	$HfB_2 + O_2 = HfO_2 + B_2O_3$		60-62	
Nitrides	BN	$4Bn + 3O_2 = 2B_2O_3 + 2N_2$	L	64,65	Liquid product B_2O_3
	TaN	$4TaN + 5O_2 = 2Ta_2O_5 + 2N_2$	P	66	
	ZrN	$2ZrN + 2O_2 = 2HfO_2 + N_2$		67	
	HfN	$2HfN + 2O_2 = 2HfO_2 + N_2$		67,68	
	TiN	$2TiN + 2O_2 = 2TiO_2 + N_2$		68	
	AlN	$4AlN + 3O_2 = 2Al_2O_3 + 2N_2$		69	Alumina former

[a]P denotes parabolic and L denotes linear.
[b]Unpublished data taken by G.C. Rybicki and J.L. Smialek of Lewis.

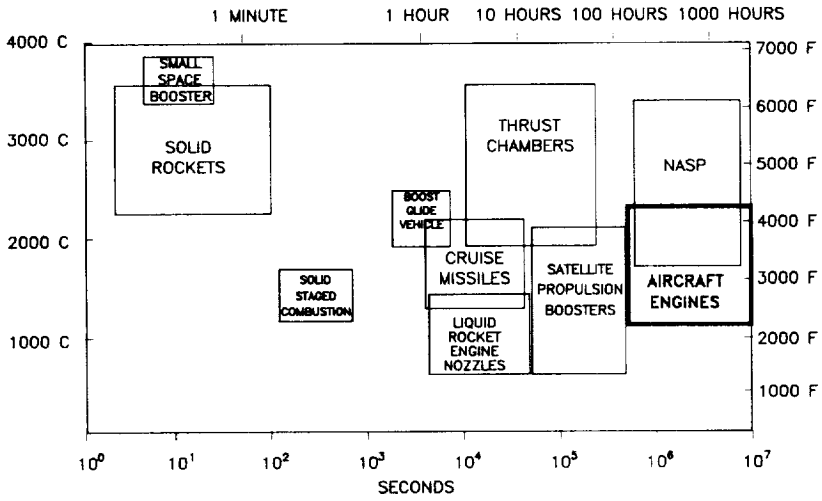

Figure 1.—Temperature-time requirements of oxidation-resistant materials for aerospace propulsion systems. (Courtesy of Aerojet General.)

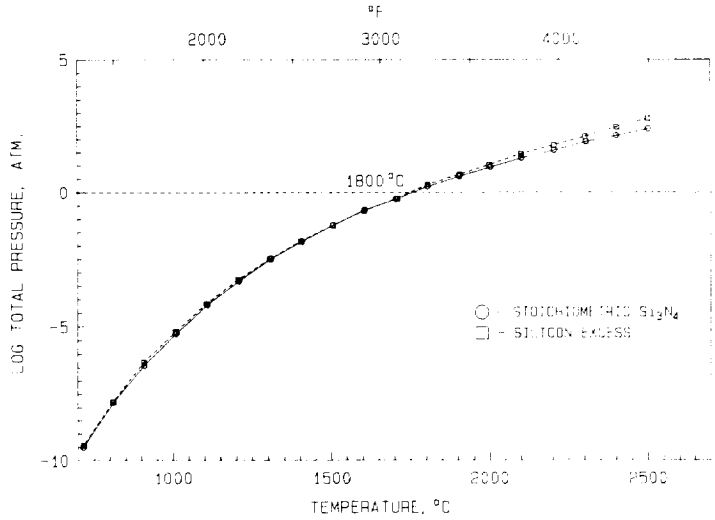

Figure 2.—Total pressure of N_2 and SiO at Si_3N_4/SiO_2 interface. (After Worrell, Wright-Patterson Program Review.)

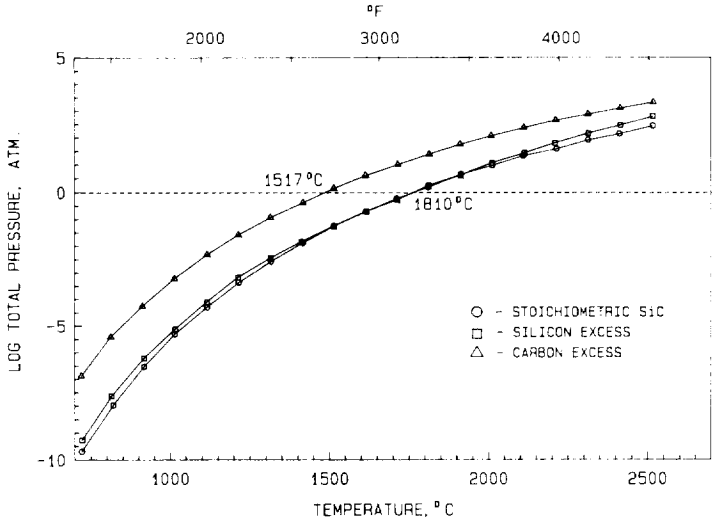

Figure 3.—Total pressure of CO and SiO at SiC/SiO_2 interface. (After Worrell, Wright-Patterson Program Review.)

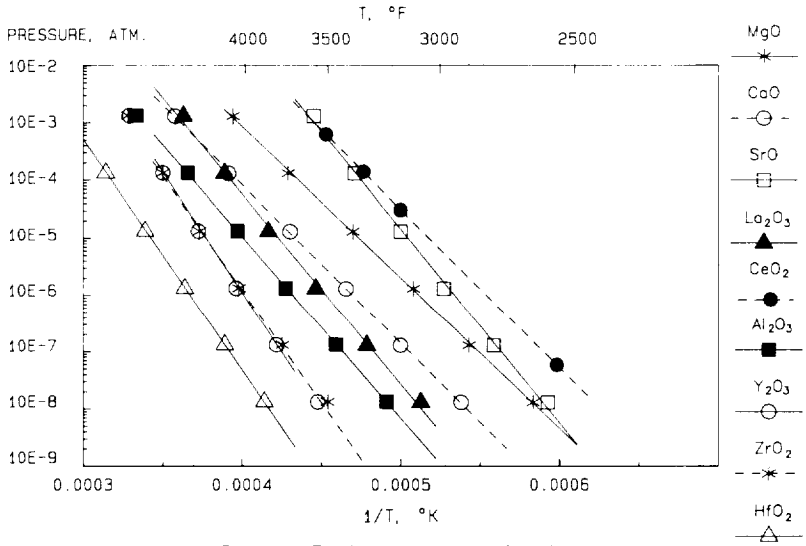

Figure 4.—Total vapor pressure of oxides.

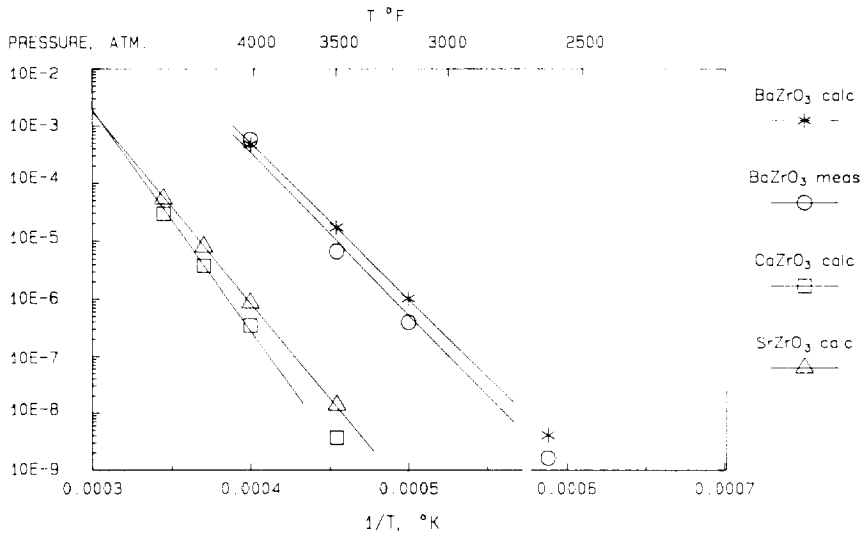

Figure 5.—Total vapor pressure of zirconates.

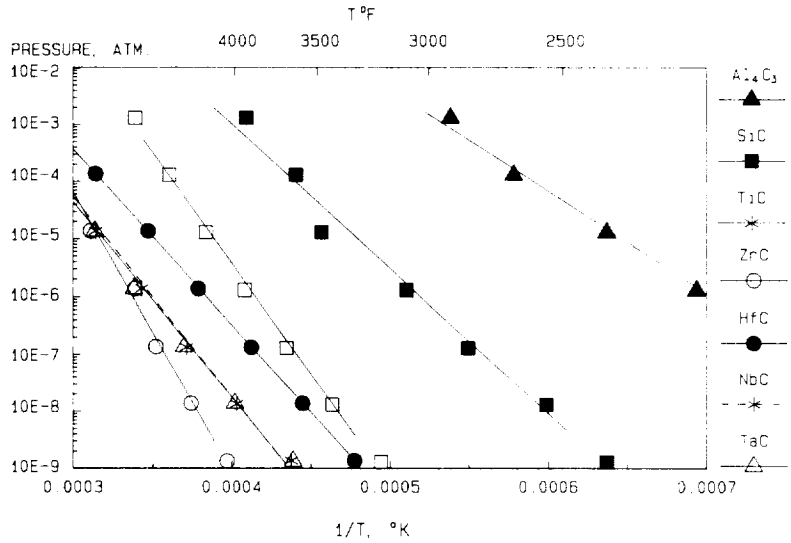

Figure 6.—Total vapor pressure of carbides.

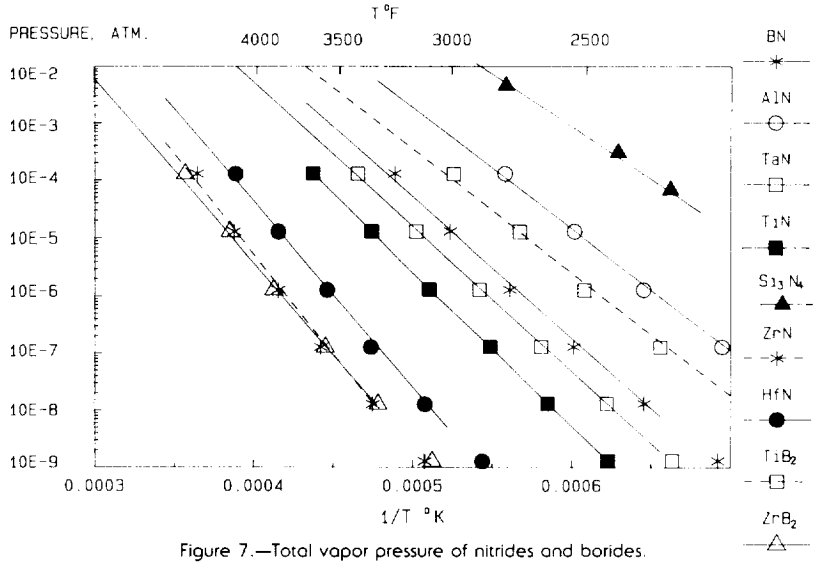

Figure 7.—Total vapor pressure of nitrides and borides.

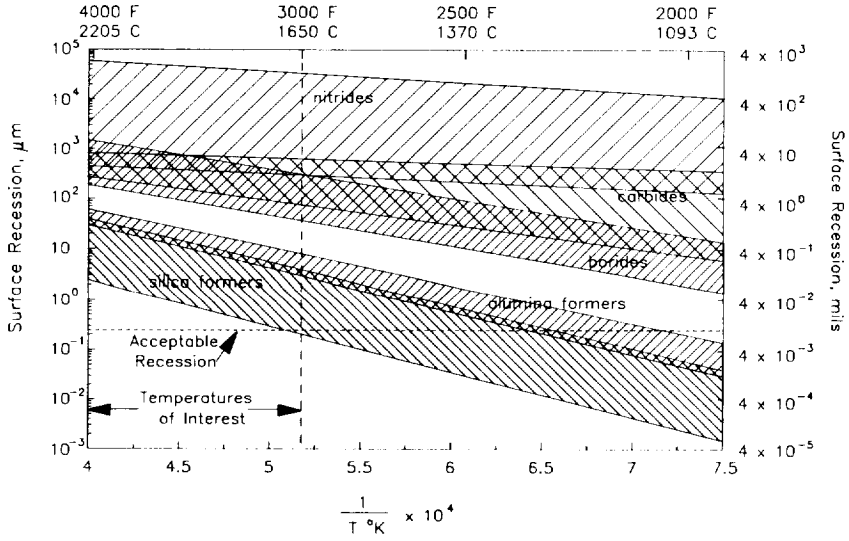

Figure 8.—Surface recession in 1 hr during isothermal oxidation.

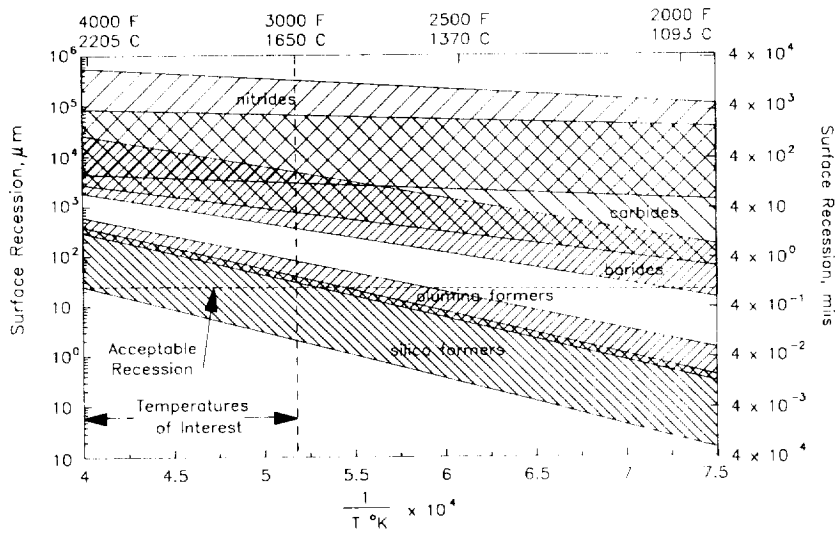

Figure 9.—Surface recession in 100 hr during isothermal oxidation

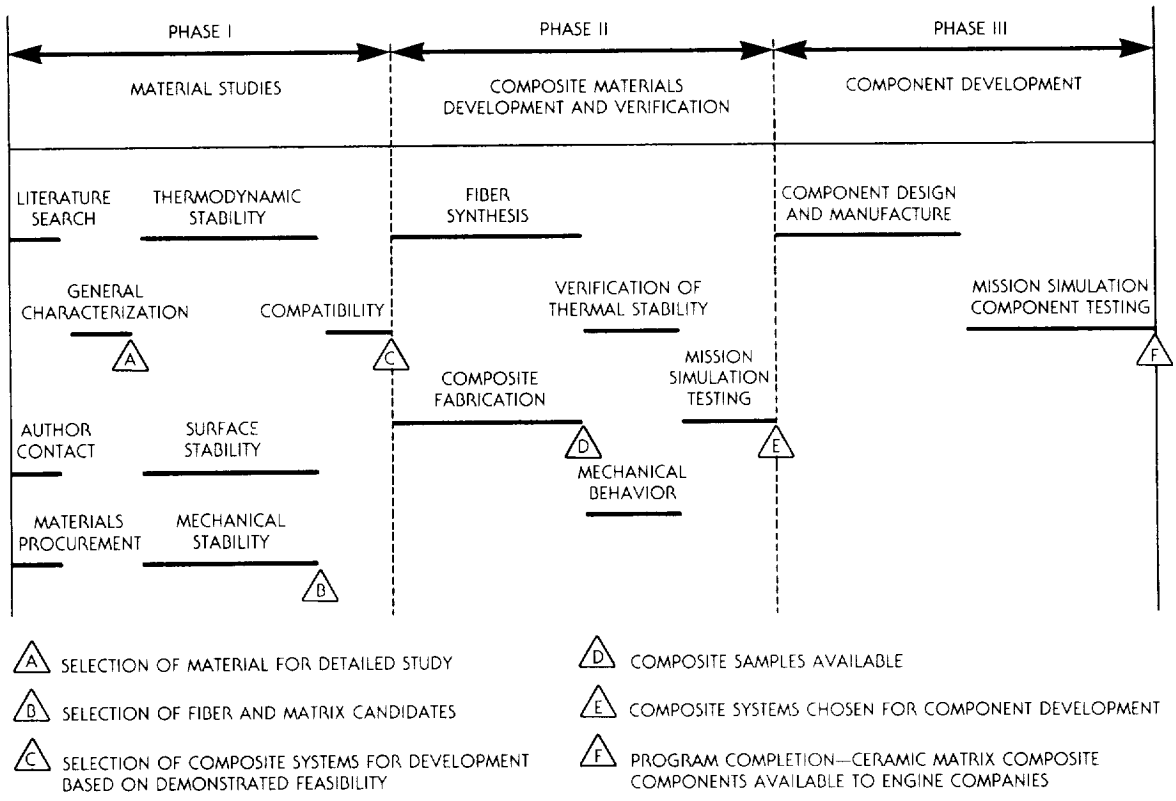

Figure 10.—Proposed program to develop ceramic matrix composites for use above 3000 °F in oxidizing aeropropulsion environments.

NASA
National Aeronautics and Space Administration

Report Documentation Page

1. Report No.	2. Government Accession No.	3. Recipient's Catalog No.
NASA TM-100169		

4. Title and Subtitle	5. Report Date
Materials for Engine Applications Above 3000 °F—an Overview	October 1987
	6. Performing Organization Code

7. Author(s)	8. Performing Organization Report No.
Nancy J. Shaw, James A. DiCarlo, Nathan S. Jacobson, Stanley R. Levine, James A. Nesbitt, Hubert B. Probst, Williams A. Sanders, and Carl A. Stearns	E-3734
	10. Work Unit No. 535-05-01

9. Performing Organization Name and Address	11. Contract or Grant No.
National Aeronautics and Space Administration Lewis Research Center Cleveland, Ohio 44135-3191	
	13. Type of Report and Period Covered Technical Memorandum

12. Sponsoring Agency Name and Address	14. Sponsoring Agency Code
National Aeronautics and Space Administration Washington, D.C. 20546-0001	

15. Supplementary Notes

16. Abstract

Materials for future generations of aeropropulsion systems will be required to perform at ever-increasing temperatures and have properties superior to the current state of the art. Improved engine efficiency can reduce specific fuel consumption and thus increase range and lower operating costs. The ultimate payoff gain is expected to come when materials are developed that can perform without cooling at gas temperatures to 2200 °C (4000 °F). This report presents an overview of materials for applications above 1650 °C (3000 °F), some pertinent physical property data, and the rationale used (1) to arrive at recommendations of material systems that qualify for further investigation, and (2) to develop a proposed plan of research. From an analysis of available thermochemical data it was concluded that such materials systems must be composed of oxide ceramics. The required structural integrity will be achieved by developing these materials into fiber-reinforced ceramic composites.

17. Key Words (Suggested by Author(s))

High-temperature ceramics
High-temperature oxides

Date for general release October 1989

Subject Category 24

19. Security Classif. (of this report)	20. Security Classif. (of this page)	21. No of pages	22. Price*
Unclassified	Unclassified	35	A03